Physics Letters B 299 (1993) 321–328
North-Holland

PHYSICS LETTERS B

A renormalization group invariant line and an infrared attractive top–Higgs mass relation

B. Schrempp [1]
Christian-Albrechts-Universität zu Kiel, W-2300 Kiel, FRG

and

F. Schrempp
Deutsches Elektronen Synchrotron – DESY, W-2000 Hamburg, FRG

Received 6 November 1992

The renormalization group equations (RGEs) of the standard model at one loop in terms of the gauge couplings $g_{1,2,3}$, the top Yukawa coupling g_t and the scalar self coupling λ are reexamined. For $g_{1,2}=0$, the general solution of the RGEs is obtained analytically in terms of an interesting special solution for the ratio λ/g_t^2 as function of the ratio g_t^2/g_3^2 which (i) represents a RG invariant line which is strongly infrared attractive, (ii) interpolates all known quasi-fixed points, and (iii) is finite for large g_t^2/g_3^2 (ultraviolet limit). All essential features survive for $g_{1,2}\neq 0$. The invariant line translates into an infrared attractive top–Higgs mass relation, which e.g. associates to the top masses $m_t=130/145/200$ GeV the Higgs masses $m_H\simeq 68$–$90/103$–$115/207$ GeV, respectively.

The experimental lower bounds on the top and Higgs masses are meanwhile quite sizeable, $m_t>91$ GeV [1] and $m_H>60$ GeV [2], respectively. This implies that the top Yukawa coupling g_t as well as the square root $\sqrt{\lambda}$ of the Higgs self coupling, related to the respective masses by

$$m_t=g_t v\,,\quad m_H=\sqrt{\lambda}v\,,\quad \text{with } v\approx 174\,\text{GeV}\,, \qquad (1)$$

are competitive in size with the gauge couplings g_3, g_2 and g_1 of the $SU(3)_c\times SU(2)_L\times U(1)_Y$ standard model gauge group.

This led us to reconsider the perturbative renormalization group equations (RGE) in the standard model at one loop, in a first step *analytically* with g_3, g_t, λ as the only nonvanishing couplings, in a second step numerically including also g_1, $g_2\neq 0$. Our aim was to search for *infrared attractive RG invariant* relations among couplings such as quasi-fixed points and invariant lines etc., beyond those known already [3–5]. Throughout this paper we shall consider an evolution of the RGE from the ultraviolet (UV) region, characterized by a scale Λ within the range of physical interest, 1 TeV$<\Lambda\leqslant 10^{15}$–$10^{19}$ GeV, into the infrared (IR) region, characterized by the scale m_Z. We stop the evolution at m_Z, since g_3 eventually runs out of the region of validity of the one-loop RGEs.

After a brief recapitulation of the known quasi-fixed points [3–5] the general solution of the standard model one-loop RGEs for g_3, g_t, $\lambda\neq 0$ and g_1, $g_2=0$, $g_{u,d,s,c,b}=0$ is presented and discussed. An *invariant line* in the ratio λ/g_t^2 as a function of the ratio g_t^2/g_3^2 is found which turns out to be strongly IR attractive. This interesting solution of the RGEs actually interpolates all known quasi-fixed points [3–5]. The general solution of the RGEs is obtained in analytical form in terms of this invariant line solution. Finally, the main features turn out to remain unaltered, if the electroweak gauge couplings g_1, g_2 are switched on. The resulting invariant line may be immediately translated into an IR attractive top–Higgs mass relation.

Let us start by acknowledging a decade of analyti-

[1] Supported by Deutsche Forschungsgemeinschaft.

cal and numerical studies of the one-loop RGEs in the presence of large Yukawa and Higgs couplings, with refs. [3–12] being the most closely related to the issues addressed in this paper. Naturally, we confirm all the known features, most importantly for our purposes:

- The "containment" of infrared m_H, m_t values within the familiar wedge [6,19] implementing the constraints from triviality and vacuum stability. The wedge is known to shrink for increasing values of the UV scale Λ, as included for illustration in fig. 1.
- The quasi-fixed points [3–5] and related numerical and analytical results [6–12].

In addition to providing new information, the analytical solution for the case g_3, g_t, $\lambda \neq 0$, $g_{1,2}=0$ will also considerably enhance the conceptual insight into the known results.

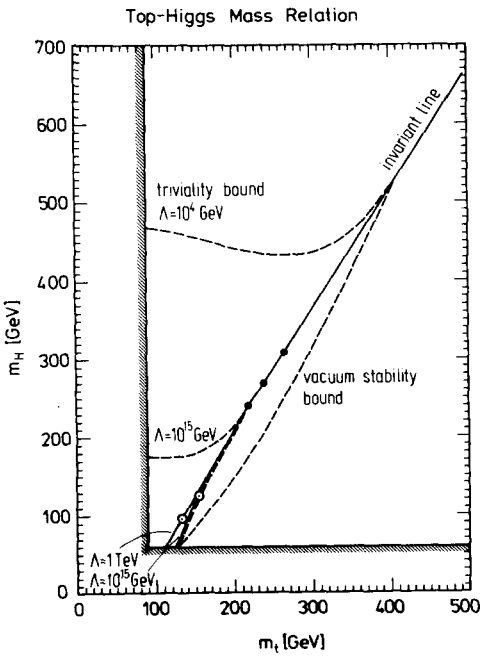

Fig. 1. The strongly IR attractive "invariant line" translated into an IR attractive top–Higgs mass relation (solid line) for two typical limiting values of Λ, $\Lambda=1$ TeV and $\Lambda=10^{15}$ GeV; the two lines coincide for $m_t \geq 170$ GeV and differ only weakly below. Also shown are the very weakly IR attractive "quasi-fixed points" (open dots), the wedges corresponding to the triviality and vacuum stability bounds for $\Lambda=10^4$ GeV and 10^{15} GeV (dashed lines), the top–Higgs mass pairs from ref. [14] (solid dots) for representative values of Λ, $10^9 \leqslant \Lambda \leqslant 10^{19}$ GeV, and the experimental bounds $m_t \geqslant 91$ GeV, $m_H \geqslant 60$ GeV.

The starting point are the one-loop RGEs for g_3, g_t, $\lambda \neq 0$ with $g_{1,2}=0$ and $g_{u,d,s,c,b}=0$

$$\frac{dg_3^2}{dt} = -\frac{7}{8\pi^2} g_3^4 , \tag{2}$$

$$\frac{dg_t^2}{dt} = \frac{1}{8\pi^2} g_t^2 (\tfrac{9}{2} g_t^2 - 8 g_3^2) , \tag{3}$$

$$\frac{d\lambda}{dt} = \frac{1}{8\pi^2} (3\lambda^2 + 6\lambda g_t^2 - 12 g_t^4) , \tag{4}$$

with $t=\frac{1}{2}\ln(Q^2/\Lambda^2)$. The general solution in the IR region, of course, depends on initial values, say, in the UV region,

$$g_{30}^2 = g_3^2(Q^2=\Lambda^2) , \quad g_{t0}^2 = g_t^2(Q^2=\Lambda^2) ,$$
$$\lambda_0 = \lambda(Q^2=\Lambda^2) , \tag{5}$$

with $1\ \text{TeV} \leqslant \Lambda \leqslant 10^{15}$–$10^{19}$ GeV.

Our primary interest is in IR stable quasi-fixed points, or, more generally, in *invariant lines* of the RGEs. According to the definition in ref. [3], a quasi-fixed point is a fixed point in a *ratio* of two couplings. In mathematical terms [13], it represents a (linear) *invariant line* in the plane of the two couplings. In this paper, we shall find a new (non-linear) invariant line in the plane of two *ratios* of couplings. The practical significance of any IR attractive quasi-fixed point or IR attractive invariant line depends on:

- The size of $\ln \Lambda/m_Z$ measuring the "length of the evolution path" from the UV to the IR region.
- The power of $(\ln \Lambda/m_Z)^{-1}$ controlling how fast the general solution (for arbitrary initial values) approaches the quasi-fixed point or invariant line.

Already in 1981 Pendleton and Ross [3] pointed out an IR attractive quasi-fixed point of eqs. (2)–(4) in the ratios g_t^2/g_3^2 and λ/g_t^2 at

$$\rho_t \equiv \frac{g_t^2}{g_3^2} = \frac{2}{9} , \quad R \equiv \frac{\lambda}{g_t^2} = \frac{\sqrt{689}-25}{4} \approx 0.31 . \tag{6}$$

This fixed point was advocated again in 1985 by Kubo, Sibold and Zimmermann [11] as a non trivial special solution of the differential equations (2)–(4) in the framework of their parameter reduction programme. The quasi-fixed point (6) corresponds (for $g_1, g_2=0$) to $m_t \approx 100$ GeV and $m_H \approx 56$ GeV. Unfortunately, it is approached exceedingly slowly, as may

be read off the general solution [4] of eqs. (2), (3), given in terms of the initial values g_{30}^2 and g_{t0}^2 or rather $\rho_{t0}=g_{t0}^2/g_{30}^2$,

$$\rho_t=\frac{2}{9}\frac{1}{1+(g_{30}^2/g_3^2)^{1/7}(2/9\rho_{t0}-1)}, \tag{7}$$

with

$$g_3^2=\frac{g_{30}^2}{1+(7/16\pi^2)g_{30}^2\ln(Q^2/\Lambda^2)}, \tag{8}$$

where $g_3^2=g_3^2(t)$ and $\rho_t=\rho_t(g_3^2(t))$, $t=\frac{1}{2}\ln(Q^2/\Lambda^2)$. The rate of approach to $\rho_t=\frac{2}{9}$ in eq. (7) for $Q^2\to m_Z^2$ is controlled by $[g_{30}^2/g_3^2(t)]^{1/7}$, which – due to the forbiddingly small power – evolves e.g. from $\Lambda=10^{15}$ GeV to m_Z only from 1 to 0.8. In fact, as was pointed out in ref. [4], for all initial values $\rho_{t0}\gg\frac{2}{9}$ a ratio

$$\rho_t\approx\frac{2/9}{1-(g_{30}^2/g_3^2)^{1/7}}\approx 1.1 \text{ for } \Lambda\approx 10^{15}\text{ GeV},$$

$$\approx 5.7 \text{ for } \Lambda\approx 1\text{ TeV}, \tag{9}$$

substantially larger than $\frac{2}{9}$ is reached in the IR, independently of ρ_{t0}. On the basis of this observation, Hill [4] solved the differential equation (3) with an appropriately defined average for g_3^2 with the result of approximating ρ_t by a Λ-dependent effective quasi-fixed point

$$\rho_t\approx\frac{14}{9}\frac{1}{\ln(g_3^2/g_{30}^2)}$$

valid for initial values satisfying

$$\tfrac{9}{2}\rho_{t0}[(g_3^2/g_{30}^2)^{1/7}-1]\gg 1. \tag{10}$$

A realization thereof may be found in the scenario of electroweak symmetry breaking through top quark condensation recently proposed by Bardeen, Hill and Lindner [14]. The resulting Λ-dependent values for the top quark mass are included for illustration in fig. 1, they lie typically well above 200 GeV.

Finally, an interesting IR stable quasi-fixed point of eqs. (2)–(4) has been pointed out by Wetterich [5] in 1987 for $g_3=0$ which is the appropriate limit for very large couplings $g_t^2, \lambda\gg g_3^2$, i.e. for very large top and Higgs masses,

$$R\equiv\frac{\lambda}{g_t^2}=\frac{\sqrt{65}-1}{4}\approx 1.77, \tag{11}$$

implying a ratio $m_H/m_t=\sqrt{R}\simeq 1.33$.

In summary, the various IR attractive fixed points for $\rho_t=g_t^2/g_3^2$ and/or $R=\lambda/g_t^2$, given in eqs. (6), (10), (11), correspond to interesting but rather strongly differing values for the top and/or Higgs mass or their ratio.

Next, let us show that they are all special points on an invariant line in λ/g_t^2 as function of g_t^2/g_3^2, which will translate into the top–Higgs mass relation advocated in this paper.

First, we observe that the three one-loop RGEs (2)–(4) may be rewritten in a *decoupled* form

$$\frac{dg_3^2}{dt}=-\frac{7}{8\pi^2}g_3^4, \tag{12}$$

$$-14g_3^2\frac{d\rho_t}{dg_3^2}=\rho_t(9\rho_t-2), \tag{13}$$

$$(9\rho_t-2)\frac{dR}{d\rho_t}=6R^2+\left(3+\frac{16}{\rho_t}\right)R-24, \tag{14}$$

with $\rho_t=g_t^2/g_3^2$ and $R=\lambda/g_t^2$. This is achieved by following a standard procedure in solving a system of coupled differential equations [13] involving the same variable (t): eq. (13) is obtained by eliminating dt from eqs. (2), (3) (valid with the possible exception of the "point" $g_3^2=0$), eq. (14) is obtained from eq. (4) by first using eq. (2) to eliminate dt in favour of dg_3^2, then eq. (13) to eliminate dg_3^2 in favour of $d\rho_t$ (valid with possible exception of the "point" $\rho_t=\frac{2}{9}$). The solutions of the three decoupled equations (12)–(14) will exhibit an increasing degree of nesting in their dependence on the original variable $t=\frac{1}{2}\ln(Q^2/\Lambda^2)$,

$$g_3^2=g_3^2(t), \quad \rho_t=\rho_t(g_3^2(t)),$$

$$R=R(\rho_t(g_3^2(t))). \tag{15}$$

The initial values, entering the general solution are g_{30}, g_{t0}, λ_0 or rather g_{30}^2, $\rho_{t0}=g_{t0}^2/g_{30}^2$ and $R_0=\lambda_0/g_{t0}^2$. Remember that ρ_t determines the top mass and R the ratio m_H^2/m_t^2 at the appropriate infrared scale. The general solutions of eqs. (12), (13) have been given already in eqs. (7), (8). It remains to solve the Riccati differential equation (14).

The most important observation is that eq. (14) has a *special solution* $\bar{R}(\rho_t)$ *which is independent of the initial values* ρ_{t0} *and* R_0, it is, instead, determined by the

boundary condition of regularity for $\rho_t \to \infty$. (16)

This solution is in mathematical terminology [13] the announced (non linear) *invariant line* in $R=R(\rho_t)$ or λ/g_t^2 as function of g_t^2/g_3^2, which plays the key role in this paper. In a forthcoming publication [15] we show that there is exactly one solution satisfying the condition (16) for R, $\rho_t \geq 0$. The limit $\rho_t = g_t^2/g_3^2 \to \infty$ corresponds to $g_t^2 \to \infty$ or $g_3^2 \to 0$, i.e. to the UV limit (for $\rho_{t0} > \frac{2}{9}$). Thus, in physical terms, $\bar{R}(\rho_t)$ is the only special solution of the RGEs with a *finite* ratio λ/g_t^2 in the UV limit.

$\bar{R}(\rho_t)$ can be represented by infinite series expansions in powers of ρ_t around $\rho_t = 0$, of $\rho_t - \frac{2}{9}$ around $\rho_t = \frac{2}{9}$ and of $1/\rho_t$ around $\rho_t = \infty$ with overlapping regions of validity

$\rho_t = 0$:

$$\bar{R}(\rho_t) = \tfrac{4}{3}\rho_t + \tfrac{2}{5}\rho_t^2 - \tfrac{7}{33}\rho_t^3 - \tfrac{79}{165}\rho_t^4 \ldots ,$$

$\rho_t = \frac{2}{9}$:

$$\bar{R}(\rho_t) = \frac{\sqrt{689}-25}{4} + 27\frac{\sqrt{689}-25}{\sqrt{689}-3}\left(\rho_t - \tfrac{2}{9}\right) + \ldots ,$$

$\rho_t \to \infty$:

$$\bar{R}(\rho_t) = \frac{\sqrt{65}-1}{4} - \frac{4}{3}\frac{\sqrt{65}-1}{\sqrt{65}+3}\frac{1}{\rho_t} + \frac{8}{9}\frac{85+11\sqrt{65}}{417+55\sqrt{65}}\frac{1}{\rho_t^2} - \ldots . \quad (17)$$

Further expansion coefficients and the regions of validity will be presented in ref. [15]. As may be read off the expansions (17), $\bar{R}(\rho_t)$ starts at the fixed point $\rho_t = 0$, $R = 0$, passes for $\rho_t = \frac{2}{9}$ through the Pendleton–Ross quasi-fixed point (6), viz. the Kubo–Sibold–Zimmermann solution, and approaches in the limit $\rho_t \to \infty$ the Wetterich quasi-fixed point (11); this is indeed the appropriate limit, since $g_3 \to 0$ translates through $\rho_t = g_t^2/g_3^2$ into $\rho_t \to \infty$. In accord with the boundary condition (16), the *finite* value $\bar{R}_\infty = (\sqrt{65}-1)/4 \approx 1.77$ is reached for $\rho_t \to \infty$. $\bar{R}(\rho_t)$ also interpolates the effective quasi-fixed points (10) at $\rho_t \geq O(1)$ for varying values of Λ (cf. also ref. [7]).

A solution similar in structure as $\bar{R}$ for large ρ_t was also discussed in ref. [9] in the different context of RGEs for extra heavy fermion doublets without mass splitting.

Before presenting and discussing the general analytical solution of eq. (14), we display in fig. 2 the RG flow, i.e. the numerical solutions of eq. (14) for various representative pairs of initial values (ρ_{t0}, R_0). The arrows show the direction of flow from the UV to the IR regime. From fig. 2 one may infer the most important properties, which will be supported and further enlightened by the analytical discussion:

(i) $\bar{R}(\rho_t)$ is indeed the *only solution* which is *regular* (*finite*) for $\rho_t \to \infty$ and, as it turns out, for $\rho_t \to 0$.

(ii) $\bar{R}(\rho_t)$ is an *invariant line*, i.e. the evolution (from UV to IR) starting *anywhere* on $\bar{R}(\rho_t)$ proceeds *along* $\bar{R}(\rho_t)$ *for all* g_3^2 or equivalently, for all choices of g_{30}^2 and Λ; the evolution continues very slowly towards the Pendleton–Ross quasi-fixed point (6).

(iii) Any other solution is first rapidly attracted towards the invariant line $\bar{R}(\rho_t)$, then it continues (very slowly) along the line towards the Pendleton–Ross quasi-fixed point. Thus, in contrast to the Pendleton–Ross quasi-fixed point, *the invariant line* $\bar{R}(\rho_t)$ *is strongly IR attractive*. This will be quantified later on.

All these features and many more may be read off the general solution of the Riccati differential equation (14), which is given in terms of the special solution

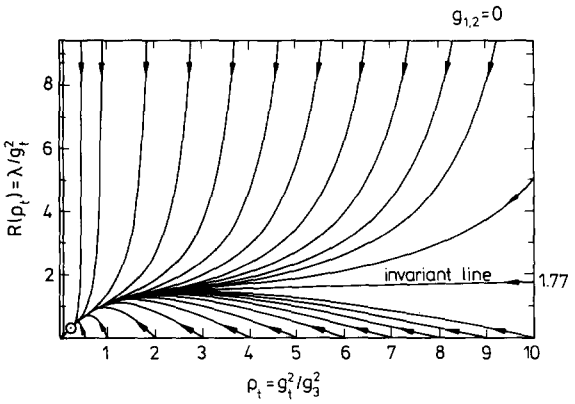

Fig. 2. One-loop renormalization group flow (with arrows pointing towards the IR) of $R=\lambda/g_t^2$ as function of $\rho_t = g_t^2/g_3^2$, in the approximation $g_{1,2}=0$. The invariant line and the strong IR attraction towards it become apparent. The invariant line obviously interpolates the very weakly IR attractive quasi-fixed point [3] at $\rho_t = \frac{2}{9}$, $R \approx 0.31$ (open dot) as well as the quasi-fixed point [5] $R = (\sqrt{65}-1)/4 \approx 1.77$ valid in the limit $g_3^2 = 0$, which is reached for $\rho_t \to \infty$.

$\bar{R}(\rho_t)$ and the pair of initial values ρ_{t0}, R_0 in analytical form as follows:

$$R(\rho_t)=\bar{R}(\rho_t)+(R_0-\overline{R_0})\exp[-F(\rho_t,\rho_{t0})]\times\left(1+\tfrac{2}{3}(R_0-\overline{R_0})\int_{\rho_t}^{\rho_{t0}}\mathrm{d}\rho_t'\frac{\exp[-F(\rho_t',\rho_{t0})]}{\rho_t'-\frac{2}{9}}\right)^{-1}, \tag{18}$$

with $R_0=R(\rho_{t0})$, $\overline{R_0}=\bar{R}(\rho_{t0})$ and

$$F(\rho_t,\rho_{t0})=\tfrac{1}{3}\int_{\rho_t}^{\rho_{t0}}\frac{\mathrm{d}\rho_t'}{\rho_t'-\frac{2}{9}}\left(4\bar{R}(\rho_t')+1+\frac{16}{3}\frac{1}{\rho_t'}\right). \tag{19}$$

A detailed analytical discussion of this general solution is deferred to ref. [15]. Let us only summarize the important results. The difference of the general and the special solution, $R(\rho_t)-\bar{R}(\rho_t)$, is given by the second term on the RHS of eq. (18), which in turn is controlled by the exponential $\exp[-F(\rho_t,\rho_{t0})]$ in the numerator and denominator. If the initial value R_0 happens to lie on the invariant line, i.e. if $R_0=\overline{R_0}$, then clearly $R(\rho_t)=\bar{R}(\rho_t)$, confirming observation (ii) above. eqs. (7), (8) tell us that for the evolution from the UV to the IR, ρ_t evolves towards $\rho_t=\frac{2}{9}$ from below, if $\rho_{t0}<\frac{2}{9}$, and from above, if $\rho_{t0}>\frac{2}{9}$; in both cases, $F(\rho_t,\rho_{t0})$ is positive and increases for increasing evolution path; this confirms the IR attractiveness of the invariant line (point (iii) above). For the discussion of the rate of attraction let us distinguish two cases:

Case 1. $R_0-\overline{R_0}$ sufficiently small, such that the denominator of eq. (18) remains close to one; the rate of approach to the invariant line is then given by $\exp[-F(\rho_t,\rho_{t0})]$ in the numerator with a behaviour for ρ_t, ρ_{t0} close to $\frac{2}{9}$:

$$\exp[-F(\rho_t,\rho_{t0})]\approx\left(\frac{\rho_t-\frac{2}{9}}{\rho_{t0}-\frac{2}{9}}\frac{\rho_{t0}}{\rho_t}\right)^{\sqrt{689}/3}=\left(\frac{g_{30}^2}{g_3^2}\right)^{\frac{1}{7}\sqrt{689}/3}=\left[1+\frac{7}{16\pi^2}g_{30}^2\ln\left(\frac{Q^2}{\Lambda^2}\right)\right]^{\sqrt{689}/21}, \tag{20}$$

with the high power $\sqrt{689}/3\approx 8.75$ beating the forbiddingly low power $\frac{1}{7}$ in eq. (7); and for ρ_t, $\rho_{t0}\geqslant$ O(1)

$$\exp[-F(\rho_t,\rho_{t0})]\approx\left(\frac{\rho_t-\frac{2}{9}}{\rho_{t0}-\frac{2}{9}}\right)^{\sqrt{65}/3}\approx\left(\frac{g_{30}^2}{g_3^2}\right)^{\frac{1}{7}\sqrt{65}/3}\rho_{t0}^{-\sqrt{65}/3}\overset{\rho_{t0}\to\infty}{\Rightarrow}0, \tag{21}$$

with a strong rate of IR attraction for sufficiently large ρ_{t0}. This is the rate controlling the approach to the effective quasi-fixed point (10) on $\bar{R}(\rho_t)$.

Case 2. If $R_0-\overline{R_0}$ becomes larger, the IR attraction towards $\bar{R}(\rho_t)$ is *strongly* enhanced, due to the substantial increase of the denominator in solution (18). Even for $R_0\to\infty$ (which, of course, is only of mathematical interest since it leads out of the range of validity of perturbation theory) the general solution $R(\rho_t)$ is attracted towards $\bar{R}(\rho_t)$ to within a *finite* difference

$$R_0\to\infty:\quad R(\rho_t)-\bar{R}(\rho_t)\to\tfrac{3}{2}\exp[-F(\rho_t,\rho_{t0})]\times\left(\int_{\rho_t}^{\rho_{t0}}\frac{\mathrm{d}\rho_t'}{\rho_t'-\frac{2}{9}}\exp[-F(\rho_t',\rho_{t0})]\right)^{-1}, \tag{22}$$

which shrinks for increasing evolution path, again controlled by $\exp[-F(\rho_t,\rho_{t0})]$. In the formal limit $\Lambda\to\infty$, which again is of academic interest only, the difference (22) shrinks to zero. Eq. (22) is, of course, the mathematical expression for the "triviality bound" for Higgs mass values in the wedge of fig. 1, which shrinks with increasing Λ.

Finally, let us point out an equivalent way of phrasing our results: the ratio $R(\rho_t)/\bar{R}(\rho_t)$ has a strongly IR attractive fixed point at 1.

Next, we switch on the electroweak gauge interactions, g_1, $g_2\neq 0$. In this letter, we only summarize the input and the results. For a state of the art mathematical treatment we refer to ref. [15]. The one-loop RGEs (2)–(4) obtain additional terms on the right-hand sides and are supplemented by the one-loop RGEs for $g_1(t)$ and $g_2(t)$

$$\frac{\mathrm{d}g_1^2}{\mathrm{d}t}=\frac{41}{48\pi^2}g_1^4,\quad \frac{\mathrm{d}g_2^2}{\mathrm{d}t}=-\frac{19}{48\pi^2}g_2^4. \tag{23}$$

By introducing the experimentally known values $\alpha(m_Z^2)=\frac{1}{128}$, $\sin^2\theta_w(m_Z^2)=0.23$, $\alpha_s(m_Z^2)=g_3^2(m_Z^2)/4\pi=0.12$, $m_Z=91.18$ GeV, one may reexpress the solutions g_1^2 and g_2^2 of eqs. (23) as functions of $g_3^2(t)$ (within the range of validity of one-loop perturbation theory) as follows:

$$\rho_1(g_3^2) \equiv \frac{g_1^2(g_3^2)}{g_3^2} = \frac{1}{8.491 g_3^2 - \frac{41}{42}},$$

$$\rho_2(g_3^2) \equiv \frac{g_2^2(g_3^2)}{g_3^2} = \frac{1}{2.043 g_3^2 + \frac{19}{42}}. \quad (24)$$

For $g_{1,2} \neq 0$, the differential equations (13) and (14) are then to be replaced by

$$-14 g_3^2 \frac{\mathrm{d}\rho_t}{\mathrm{d}g_3^2} = \rho_t^2 \left(9 - \frac{2}{\rho_t} - \frac{17}{6}\frac{\rho_1}{\rho_t} - \frac{9}{2}\frac{\rho_2}{\rho_t}\right), \quad (25)$$

$$-14 g_3^2 \frac{\mathrm{d}R}{\mathrm{d}g_3^2} = \rho_t \left[6R^2 + \left(3 + \frac{16}{\rho_t} - \frac{1}{6}\frac{\rho_1}{\rho_t} - \frac{9}{2}\frac{\rho_2}{\rho_t}\right) R - 24 + \frac{3}{2}\frac{\rho_1^2}{\rho_t^2} + 3\frac{\rho_1\rho_2}{\rho_t^2} + \frac{9}{2}\frac{\rho_2^2}{\rho_t^2}\right]. \quad (26)$$

The explicit dependence on g_3^2, introduced by the ρ_1, ρ_2 terms, cannot be eliminated anymore. However, we see immediately that the $\rho_{1,2}$ dependence enters in the form of the ratios $\rho_{1,2}/\rho_t$. As long as $\Lambda \leqslant 10^{15}$–$10^{19}$ GeV, we have $\rho_{1,2} \leqslant O(1)$; hence one expects the $\rho_{1,2}$ dependence to become negligible for large values of ρ_t, which will be borne out by our numerical calculations. It is sizeable only for small values of ρ_t, which fortunately are already excluded by the experimental lower bounds on m_t and m_H.

The system of differential equations for ρ_1, ρ_2, ρ_t and R as functions of g_3^2 has a fixed point at $\rho_{1,2}=0$, $\rho_t = \frac{2}{9}$, $R = (\sqrt{689}-25)/4$. Following ref. [13], we solve the linearized system in the neighborhood of this fixed point analytically [15] and find the following:

(i) Only for initial values $\rho_{t0} \approx \frac{2}{9} - \frac{1}{324}(17\rho_{10} + 27\rho_{20})$, one is driven to the solution advocated in ref. [11], which leads to $m_t \simeq 95$ GeV and $m_H \simeq 65$ GeV, values which are close to the present experimental bounds.

(ii) Else, any solution is again *strongly* attracted by an effective "invariant line" and *very weakly* by an effective "fixed point" on this line, the $g_{1,2} \neq 0$ generalization of the Pendleton–Ross fixed point (6). Given an evolution from $Q^2 = \Lambda^2$ to $Q^2 = m_Z^2$, the "invariant line" is the locus of all *endpoints* of this evolution for *all starting points* on and sufficiently close to this line. The location of this "invariant line" in the $R - \rho_t$ plane depends on Λ: however, the important point is that for any Λ, 1 TeV $\leqslant \Lambda \leqslant 10^{15}$–$10^{19}$ GeV, the Λ-dependence disappears for $\rho_t \geqslant 0.8$ and is *only weak* for $\rho_t \leqslant 0.8$. More precisely, for $\rho_t \geqslant 0.8$ all Λ-dependent "invariant lines" merge with the genuine invariant line of the $g_{1,2}=0$ case; for $\rho_t \leqslant 0.8$ the Λ-dependence remains weak as long as one remains within the region of R, ρ_t values admitted by the present experimental lower bounds on m_t and m_H. This justifies *a posteriori* the term "invariant line" in quotes; it is an effective invariant line in a similar sense as the effective quasi-fixed point (10). On each "invariant line" lies the announced effective Λ-dependent "fixed point", defined as the point in the R–ρ_t plane where the starting point and the end point of the evolution from Λ to m_Z coincide. To quantify the Λ-dependence, we choose two physically motivated extremal values for Λ, $\Lambda = 1$ TeV and $\Lambda = 10^{15}$ GeV; the corresponding two "invariant lines' may be considered as limiting "invariant lines". For a figure we refer to ref. [15].

Finally, let us translate these two limiting "invariant lines" for $\Lambda = 1$ TeV and 10^{15} GeV into limiting relations between the physical parameters m_H and m_t using

$$m_H = \sqrt{\bar{R}\rho_t g_3^2}\,|_{\sqrt{Q^2}=m_H} \cdot 174 \text{ GeV},$$

$$m_t = \sqrt{\rho_t g_3^2}\,|_{\sqrt{Q^2}=m_t} \cdot 174 \text{ GeV}. \quad (27)$$

The resulting *infrared attractive top–Higgs mass relations* are displayed in fig. 1 for $m_t \leqslant 500$ GeV (solid lines). The experimental lower bounds, 60 GeV for m_H and 91 GeV for m_t, the boundary wedges for $\Lambda = 10^4$ GeV and 10^{15} GeV (dashed lines) and the values of the top and Higgs masses obtained in the framework of the BHL top condensation model [14] for various values of Λ (solid dots), are shown as well. The Λ dependent "fixed points" (open dots) are also included.

The most recent indirect experimental information on the top mass from LEP and other precision experiments amounts to [2]

$$\text{all data}\,|_{m_H \simeq 300\,\text{GeV}}: \; m_t = 145^{+17}_{-19} \text{ GeV}, \quad (28)$$

and to [16]

$$\text{all data}\,|_{m_H = m_Z}: \; m_t = 132^{+24}_{-26} \text{ GeV}, \quad (29)$$

$$\text{all data}\,|_{m_H \text{ free}}: \; m_t = 124^{+26}_{-28} \text{ GeV},$$

$$m_H = 25^{+275}_{-19} \text{ GeV}. \quad (30)$$

Let us therefore quote some representative values, read off the two limiting top–Higgs mass relations in fig. 1, within the region of special interest, $91 \leqslant m_t \leqslant 200$ GeV,

$$\text{for } m_{H\min} = 60 \text{ GeV}, \quad m_t \simeq 112\text{–}125 \text{ GeV},$$

$$\text{for } m_t = 130 \text{ GeV}, \quad m_H \simeq 68\text{–}90 \text{ GeV},$$

$$\text{for } m_t = 145 \text{ GeV}, \quad m_H \simeq 103\text{–}115 \text{ GeV},$$

$$\text{for } m_t = 200 \text{ GeV}, \quad m_H \simeq 207 \text{ GeV}. \tag{31}$$

The locations of the effective Pendleton–Ross "fixed points" for the two chosen extremal values of the cut-off scale Λ are

$$m_H = 97 \text{ GeV}, \quad m_t = 134 \text{ GeV},$$

$$\text{for } \Lambda = 1 \text{ TeV},$$

$$m_H = 126 \text{ GeV}, \quad m_t = 155 \text{ GeV},$$

$$\text{for } \Lambda = 10^{15} \text{ GeV}. \tag{32}$$

Of course, the top–Higgs mass relation in fig. 1 and the mass values in eqs. (31), (32) depend somewhat on the chosen values for $\alpha_s(m_Z^2)$, $\sin^2\theta_w(m_Z^2)$, $\alpha(m_Z^2)$ and m_Z.

It is furthermore very instructive to discuss the behaviour of the boundary wedge as function of Λ in relation to the invariant line (cf. fig. 2). For a given value of Λ the boundary wedge consists of two well-known branches [6,10], the triviality bound (bounding m_H from above) and the vacuum stability bound (bounding m_t from above). The two branches meet at the tip of the wedge. The tip (i) collects the IR images of the UV points with $\rho_{t0} \gg \frac{2}{9}$, i.e. it coincides with the effective quasi-fixed point (10), (ii) it correspondingly coincides with the pair of top–Higgs masses obtained in the BHL top condensation approach [14], and (iii) it lies on the invariant line. For increasing values of Λ, the tip of the wedge slides down the invariant line. For $\Lambda = 10^4$ GeV the two branches of the wedge are – apart from the tip region – well distinct from the invariant line. For increasing Λ they are attracted towards it. For $\Lambda = 10^{15}$ GeV the vacuum stability bound has essentially reached the invariant line, which increases its significance. This is not the case for the triviality bound, which collects IR images of UV points with very large R_0 and small ρ_{t0}; it continues to shrink towards the invariant line for increasing Λ.

The physical significance of the essentially Λ independent IR attractisve top–Higgs mass relation has to be judged according to the usual criteria applied to fixed point structures: it is the more significant the longer the evolution path is, measured by $\ln \Lambda/m_Z$, and the stronger the rate of attraction towards it. The rate of attraction has been shown to be strong indeed (in contradistinction to that of the Pendleton–Ross quasi-fixed point). For large values of Λ, e.g. in grand unified theories with $\Lambda \sim 10^{15}$ GeV, all UV points admitted within one-loop perturbation theory, except those pairs R_0, ρ_{t0} with R_0 large and ρ_{t0} small, evolve into IR points on or fairly close to the top–Higgs mass relation in fig. 1 (for a quantification see ref. [15]).

In this context a more speculative but quite attractive suggestion [17,11] is worth recalling: parameters like renormalized couplings (masses, ...) of the standard model in the IR regime ($\sqrt{Q^2} \approx m_Z$) might well be selfconsistently determined such as to cancel their sensitivity to the UV regime ($\sqrt{Q^2} \approx \Lambda$), the presumed onset of new unknown physics. A well-defined realization of these ideas is to tune the parameters onto IR attractive quasi-fixed point or invariant line solutions of the RGEs. The IR attractive top–Higgs mass relation in fig. 1 is precisely of this kind, the Pendleton–Ross "fixed point" (32) even more so.

Finally, let us speculate on the limit of possibly very large top and Higgs masses, outside the range of validity of perturbation theory. We remember that the advocated invariant line is the *only* solution of the one-loop RGEs which tends to a *finite ratio* for λ/g_t^2 in the formal UV limit of large g_t^2/g_3^2. Thus, it is near at hand to suggest (cf. also ref. [5]) that it might continue to be approximately valid in the non-perturbative regime of large g_t^2, λ. First results in lattice Higgs–Yukawa models [18] actually tend to confirm this suggestion. In other words, if there is any "escape route" from the perturbative triviality and vacuum stability bounds, it is presumably along the invariant line through the tip of the boundary wedge.

We thank J. Bartels, J. Ellis, M. Lindner, K. Sibold, G. Veneziano and C. Wetterich for interesting discussions and suggestions. One of us (B.S.) is grateful to the II. Institut für Theoretische Physik, Universität Hamburg, and the DESY Theory Group for the extended hospitality. We thank the CERN Theory

Division for its hospitality during a short visit, where the paper was finalized.

References

[1] CDF Collab., F. Abe et al., Phys. Rev. D 43 (1991) 2070.
[2] L. Rolandi, plenary session talk 26th Conf. on High energy physics (Dallas, TX, 1992).
[3] B. Pendleton and G.G. Ross, Phys. Lett. 98 B (1981) 291.
[4] Ch.T. Hill, Phys. Rev. D 24 (1981) 691.
[5] C. Wetterich, Proc. Trieste HEP Workshop (1987) p. 403, and preprint DESY-87-154 (1987).
[6] L. Maiani, G. Parisi and R. Petronzio, Nucl. Phys. B 136 (1978) 115;
N. Cabbibo et al., Nucl. Phys. B 158 (1979) 295.
[7] Ch.T. Hill, C.N. Leung and S. Rao, Nucl. Phys. B 262 (1985) 517.
[8] E.A. Paschos, Z. Phys. C 26 (1984) 235.
[9] J. Bagger, S. Dimopoulos and M. Masso, Nucl. Phys. B 253 (1985) 397;
S. Dimopoulos and S. Theodorakis, Phys. Lett. B 154 (1985) 153.
[10] M. Lindner, Z. Phys. C 31 (1986) 295;
M. Lindner, M. Sher and H.W. Zaglauer, Phys. Lett. B 228 (1989) 139;
B. Grzadkowski and M. Lindner, Phys. Lett. B 178 (1986) 81; B 193 (1987) 71.
[11] J. Kubo, K. Sibold and W. Zimmermann, Nucl. Phys. B 259 (1985) 331; Phys. Lett. B 220 (1989) 185.
[12] W.J. Marciano, Phys. Rev. Lett. 62 (1989) 2793.
[13] see, e.g., J. Guckenheimer and P. Holmes, Non-linear oscillations, dynamical systems and bifurcations of vector fields, Applied Mathematical Sciences, Vol. 42 (Springer, Berlin).
[14] W.A. Bardeen, Ch.T. Hill and M. Lindner, Phys. Rev. D 41 (1990) 1647;
W.A. Bardeen, report FERMILAB-CONF-90/269-T (1990);
Ch.T. Hill, preprint FERMILAB-PUB-92-19-T (1992);
M. Lindner, Habilitation thesis, University of Heidelberg (1992).
[15] B. Schrempp and F. Schrempp, to be published.
[16] J. Ellis, G.L. Fogli and E. Lisi, Phys. Lett. B 292 (1992) 427.
[17] M. Veltman, Acta Phys. Pol. B 12 (1981) 437;
Y. Nambu, preprint EFI-89-08 (1989);
P. Osland and T.T. Wu, preprint Harvard-DAS-92/1 (1992).
[18] L. Lin, I. Montvay, G. Münster and H. Wittig, Nucl. Phys. B (Procl. Suppl.) 20 (1991) 601;
C. Frick, L. Lin, I. Montvay, G. Münster, M. Plagge, T. Trappenberg and H. Wittig, preprint DESY-92-111 (1992), and to be published.